Efficient brain conductivity and permittivity mapping using a zero TE (ZTE) acquisition

Ileana Hancu[1], Seung-Kyun Lee[1], Selaka Bulumulla[1], Laura Sacolick[2], Wei Sun[3], and Florian Wiesinger[4]
[1]GE Global Research Center, Niskayuna, NY, United States, [2]GE Healthcare, Munich, Germany, [3]GE Healthcare, Wisconsin, United States, [4]GE Global Research Center, Munich, Germany

Target Audience: Researchers/clinicians interested in brain conductivity and permittivity measurements by MRI

Introduction: Spatially resolved tissue conductivity and permittivity maps are desired in MRI for a variety of reasons, including SAR prediction at high field. The higher conductivity and permittivity of malignant tissues [1] also point to these two parameters as potentially useful markers for cancer detection and treatment monitoring. In the few mathematical formulations that enable the computation of tissue electrical properties (TEP's), a minimum of two MRI acquisitions are required to extract conductivity and permittivity: one to map the magnitude of the transmit field, and one to allow for an approximation of the phase of the transmit field. Based on a recent reformulation of Helmholtz's equations [2] and on the very desirable properties of 3D ZTE imaging, we demonstrate conductivity and permittivity mapping using a single acquisition only. A ~7 min ZTE exam, acquired at 2.2mm isotropic resolution, is shown to enable computation of full brain TEP maps at 3T.

Theory: Using an reformulation of Helmholtz's equations [2] conductivity and permittivity can be approximated according to Eqs. [1,2]. As seen in these equations, the complex values of the transceive field are the only variables needed for computing TEP maps. While the magnitude of the transceive field can be acquired efficiently using standard, low flip angle GRE scans, the object induced phase is more difficult to assess. If the phase data from the initial GRE scan is used for this purpose, two additional scans are needed, to correct for eddy currents and chemical shift induced phase changes [3]. Alternatively, an extra spin-echo scan can be used for measuring the transceive phase. We show here that 3D, ZTE imaging offers all the data needed for TEP mapping.

$$\epsilon_r \approx -\frac{1}{\mu\epsilon_0\omega^2} Re\left(\frac{\nabla^2\sqrt{B_1^+B_1^-}}{\sqrt{B_1^+B_1^-}}\right) \quad [1]$$

$$\sigma \approx \frac{1}{\mu\omega} Im\left(\frac{\nabla^2\sqrt{B_1^+B_1^-}}{\sqrt{B_1^+B_1^-}}\right) \quad [2]$$

.

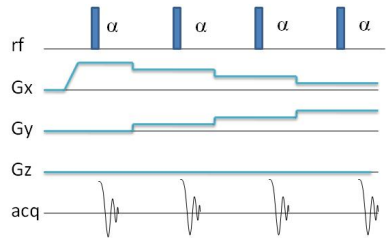

Figure 1. ZTE acquisition

Experimental: The chosen ZTE pulse sequence is depicted in Fig. 1 and it conceptually follows the implementations described in [4]. It uses 3D radial center-out k-space sampling with constant imaging gradients and no ramping, except for small incremental directional updates. With the imaging gradient present during RF excitation, the RF pulse width has to be short (<1/$BW_{readout}$), resulting in generally low flip angles. The zero TE of the sequence causes minimal phase changes due to spin dephasing under B_0 or chemical shift inhomogeneities; the limited gradient switching also causes minimal or no phase-changing eddy currents. Computation of the Laplacian was done using a quadratic fit, using 3 (phantom) and 5 (*in vivo*) additional points on each side of the pixel of interest. No additional data filtering was performed. The water based, half sphere conductivity phantom contained 3 small spheres, of ~8ml volume. The 4 compartments had conductivities of 0.16/0.65/0.87/ 1.45 S/m for the outer/bottom/middle/top compartment, respectively. These conductivity measurements were performed at 200MHz, yielding slightly larger values than the ones that would be measured at 128MHz. The imaging parameters chosen for all data acquisition are: cubical FOV = 28cm, acquisition matrix = 128pts, flip angle = 2-3º, BW=31kHz, TE=12⊠s, NEX=16, scan time ~7.2min, All experiments were performed on a 3T, Discovery MR750 scanner (GE Healthcare, Waukesha, WI) using a transmit/receive birdcage coil.

Results: Figure 2 shows one slice of the magnitude and phase of the data (1st and 2nd column, respectively), as well as the permittivity and conductivity reconstructions (3rd and 4th column, respectively) for the phantom (top) and *in vivo* experiments (bottom). Permittivity values close to the ones reported in the literature (¶$_r$~80) are obtained for the outer compartment of the phantom. Computation of a second derivative through a step function (visible in the magnitude data at the transition between compartments) leads to unrealistically high permittivity values near that transition. The smoothness of phase data among different compartments (only less than 0.01 radians difference exist between compartments) leads to good conductivity estimates. Figure 3 shows a plot relating the average MRI conductivity measurements in the 4 compartments (@ 128MHz) versus the 200MHz dielectric probe measurements. The high correlation between the two sets (r=0.998, p=0.002) points to MRI as a useful tool for non-invasive conductivity measurements. Similar conclusions apply to the in vivo data set, with image contrast having a negative impact on permittivity measurements, and the conductivity maps displaying high quality, enabling visualization of corpus callosum, white and gray matter as well as CSF, and yielding measurements very consistent with the literature.

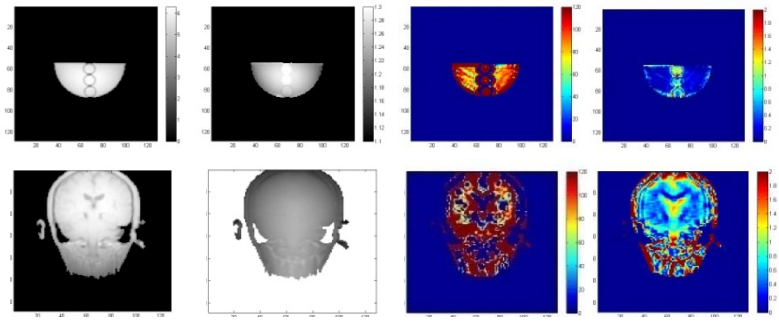

Figure 2. Magnitude, phase of the ZTE data, permittivity and conductivity maps.

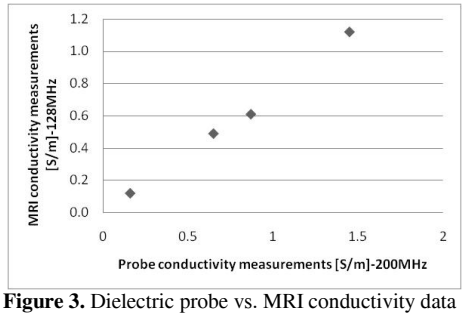

Figure 3. Dielectric probe vs. MRI conductivity data

Conclusions: A new approach was presented, allowing conductivity and permittivity mapping from a single 3D data set. Using a ZTE approach with minimal gradient switching (to reduce eddy current induced phase changes), which maximize SNR efficiency and minimizes unwanted phase changes due to chemical shift and B_0 inhomogeneities, a 3D sequence similar to the one presented here could offer an efficient and accurate way to map TEP's. Segmentation approaches may be needed for small regions of interest or high contrast images.

Acknowledgement: This work was supported by NIH grant 1R01CA154433.

References: [1] Joines et al, Med Phys 21:547 (1994) [2] Lee S-K et al, ISMRM 2013, 462 [3] van Lier et al, MRM 67: 552 (2012) [4] Madio et. MRM 34:525 (1995)